

A SET OF FINITE ELEMENTS FOR 2D ANALYSIS OF REINFORCED CONCRETE FOUNDATIONS ON DEFORMABLE SUBSOIL

Waldemar SZAJNA ¹

A b s t r a c t

The paper presents a formulation and verification of a 2D soil – structure interaction model which enables the analysis of reinforced concrete shallow foundations under monotonic short-time loads. The structure supported by a deformable subsoil, whose elasto-plastic features are being considered. The structure model describes: the ability of crack creation, non-linear stress – strain characteristics of concrete and reinforcement and also reinforcement – concrete interaction. The foundation – subsoil contact model enables the identification of slide and adhesion zones.

The presented mathematical formulation allowed for the development of a set of finite elements simulating the behaviour of the foundation, the subsoil and the contact zone between them. The elasto-plastic approach was used to describe the behaviour of the structure, the subsoil and the contact phenomena. Computer programs were prepared and verifying analyses were presented.

Keywords: Soil – structure interaction, reinforced concrete, FEM, contact element

1. INTRODUCTION

The building foundation supported by z deformable subsoil creates a problem of the soil – structure interaction (SSI). The problem is characterized by considerable differences in the values of mechanical parameters of the subsystems being in contact. Stiffness and strength of reinforced concrete foundations and subsoil differ even by several orders of magnitude, see e.g. Look [1]. The ability of concrete cracking, its non-linear stress – strain characteristics and the interaction with steel reinforcement are also a challenge. Additionally, there is a possibility of sliding and separation along the foundation – subsoil contact surface.

Depending on the subject of interest, there are two extremely different attitudes to soil – structure interaction presented in the literature. In the first attitude, typical for structural engineering, complex models of structures (taking into account e.g. stiffness degradation in a deformation process) and simplified soil models (e.g. the one-parameter Winkler's analogue) are assumed. In the other attitude, which is characteristic for geotechnical engineering, the contrary situation takes place. Complex soil

¹ Corresponding author: University of Zielona Góra, Institute of Civil Engineering, 65-516 Zielona Góra, Poland, e-mail: W.Szajna@ib.uz.zgora.pl

constitutive models (including consolidation, water drainage etc.) and simplified structure models (e.g. treated as punches) are used. The reason of this situation is the fact that structural mechanics, soil mechanics and additionally, contact mechanics are three separate wide areas of research, but related to soil – structure interaction. In this paper it is assumed that the models of the reinforced concrete structure, the subsoil and the contact area would remain at the similar order of complexity.

The behaviour of reinforced concrete and soil is often described in terms of elasto-plasticity, see e.g. Hofsetter and Mang [2], Tejchman and Bobiński [3], Chen and Mizuno [4], Yu [5], Puzrin [6]. A comprehensive review of approaches to numerical modelling of reinforced concrete can be found in [7]. Despite the considerable differences in internal structure of materials such as steel, concrete or soil, their macroscopic behaviours display similarity. They all exhibit elasticity, plasticity, brittleness, hardening, etc. although at different levels of intensity. There is also an analogy between contact friction and perfect plasticity (see Michałowski and Mróz [8]). So, the use of the elasto-plastic attitude to modelling the reinforced concrete structure, the subsoil and the contact area is justified in this study.

In modelling soil-structure interaction, much more attention is paid to constitutive models of the soil, than to contact conditions. However, the load transfer from the superstructure to the ground takes place via the contact surface and proper modelling of the contact conditions may affect significantly the analysis results. This is particularly true with cases where large concentrated loads are applied or where significant displacements tangential to the contact surface occur. The importance of the method of modelling of contact conditions and their impact on the results of numerical solutions to typical engineering problems have been presented in many works, see e.g. Potts and Zdravković [9], Sheng et al. [10] or Dhadse et al. [11].

Historically, modelling of SSI using the finite element method (FEM) was developed with the use of zero thickness contact elements introduced by Goodman et al. [12] and thin layer elements proposed by Desai, et al. [13]. Their comparison is included in Qian et al. [14] among others. Both concepts are still being developed. Modified formulations of zero thickness elements were presented by Dhadse et al. [11]. The comparison of zero thickness and continuum elements implemented in Plaxis was analysed by Damians et al. [15] who delivered element parameters that give the same numerical outcomes. A new thin-layer interface element formulation was proposed by Dalili et al. [16] and the element was used to conduct soil – framed structure interaction analysis.

A comprehensive review of the possible formulations of contact modelling was provided by: Li et al. [17], Dhadse et al. [18] and Belhadj et al. [19].

In laboratory tests of contact zones, macrostructural and microstructural approaches are distinguished. Macroscale research was conducted by Chen et al. [20] among others. They analysed surface roughness and its effect on interfacial shear behaviour of clay – concrete interface.

Microscale tests exploiting the image analysis of soil – structure interface were carried out by Zhang et al. [21]. Zhang and Zhang [22] proposed to treat the contact zone as a kind of composite, including the lower surface of the building's foundation and the layer of adjacent soil. The mechanical behaviour of this zone differs from that of the soil itself due to the constraints introduced by the presence of the structure. In the contact layer, the displacement and deformation fields are non-uniform.

Hu and Pu [23] were testing and modelling the influence of the interface surface roughness on the sand – steel contact zone. Elastic perfect-plastic failure occurs along the smooth interface, while strain localization, strain-softening and dilatancy occur on a rough interface. A damage constitutive model with ten parameters for interface was proposed.

The localized nature of the load transfer mechanism from the structure to the subsoil has limited the reliability of geotechnical predictions and design. The problem was analysed by DeJong et al. [24] using particle image velocimetry technique.

New techniques for numerical analyses have been introduced in the investigation of the soil – structure contact zone recently. For the soil domain involving large displacements, discrete element method was successfully used by Dang and Meguid [25]. For large displacement and large strain problems, the particle finite element method was used, see Carbonell et al. [26].

When analysing structural elements in building structures, it is convenient to use generalized stresses (bending moments, transverse forces) and generalized displacements (rotation angles and translation of the middle surfaces of plates and shells) to describe their behaviour. For this reason, the interface elements are intended not only to model the foundation – soil contact, but also to provide a connection between finite elements with different degrees of freedom (rotational and translational in the foundation raft and only translational in the soil).

The aim of the current work is the elaboration of a simple numerical model which would allow investigating the interaction between engineer structures and subsoil, described by a small number of standard parameters. The statics of a soil – shallow foundation structure system, subjected to monotonic short-time loads in a plane state of strains is considered. It is assumed that the reinforced concrete structure is supported by a deformable subsoil with an arbitrary system of geological layers. In practical engineering applications, it is important for the model to be described by a limited number of material parameters, values of which can be obtained in standard tests.

2. PROBLEM DEFINITION

General assumptions:

1. A continual description of materials with neglecting their internal structure has been used.
2. All the non-continuities in the system (concrete cracks, foundation slip on the surface of subsoil) are modelled by constitutive equations.
3. A homogeneous elasto-plastic description characterises the irreversible strains appearing in the reinforced concrete structure, in the subsoil and in the foundation – subsoil contact surface.
4. FEM spatial discretisation has been applied.

Fig. 1 presents a part of a hypothetical long foundation structure which is situated on a subsoil with a certain system of geological layers. A part of the ground lying in the neighbourhood of the foundation has been separated from the semi-infinite subsoil (dashed line in Fig. 1). The separated part, which has been discretised into finite elements (right side of Fig. 1), should be big enough to prevent boundary conditions from disturbing the view of the phenomena which take place in the neighbourhood of the foundation.

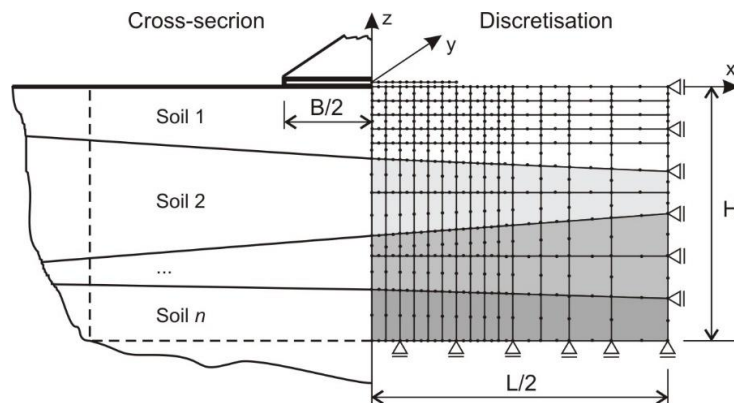


Fig. 1. A section and the FEM spatial discretisation

The foundation raft has been also discretised. An additional layer of finite elements, known as interface elements, has been introduced between the structure and the subsoil finite elements. The function of the layer is to model the phenomena taking place on the contact surface.

3. A VIRTUAL WORK EQUATION OF THE BODIES BEING IN CONTACT

The equation of the virtual work (Koiter [27]) of the bodies being in contact of a total volume V , lateral surface S and contact surface S_c takes the form

$$\int_V \delta \boldsymbol{\varepsilon}^T \boldsymbol{\sigma} dV + \int_{S_c} \delta \Delta \mathbf{u}^T \mathbf{t}_c dS_c = \int_V \delta \mathbf{u}^T \mathbf{b} dV + \int_S \delta \mathbf{u}^T \mathbf{p} dS \quad (3.1)$$

where:

$\delta \mathbf{u}, \delta \Delta \mathbf{u}, \delta \boldsymbol{\varepsilon}$ – vector of virtual displacements, vector of relative virtual displacements, tensor of virtual strains respectively,

$\boldsymbol{\sigma}, \mathbf{b}, \mathbf{p}$ – tensor of stresses, vector of body forces and vector of surface forces respectively,

\mathbf{t}_c – vector of mutual reactions on the contact surface S_c .

The first component of the left side of equation (3.1) will be used to derive the stiffness matrixes of the structure element and the subsoil element, whereas the second term to derive the stiffness matrix of the interface element.

Hypothetical two bodies a and b , subjected to surface and body forces, in contact in the S_c zone, are shown in Figure 2.

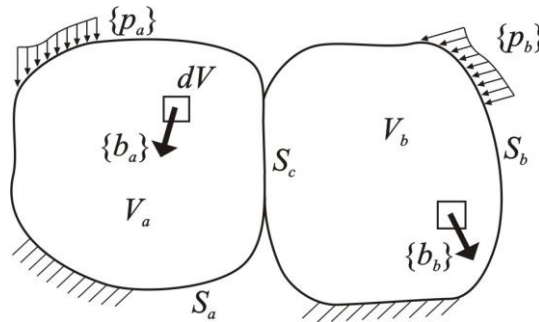


Fig. 2. Contact of bodies a and b

4. FINITE PLATE STRIP

A plate strip subjected to compression and bending to a cylindrical surface is considered. While bending, the change of the curvature $\left(\frac{dw}{dx}\right)$ as well as strains (β) caused by the shear forces are taken into account, according to Mindlin's hypothesis, Owen and Figueiras, [28] – Fig. 3.

So, it is assumed that a section which is flat before deformation remains flat after it, but the section is not normal to the midsurface.

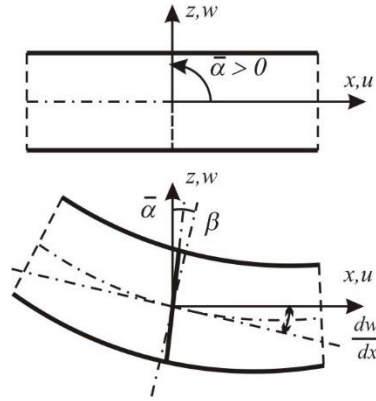


Fig. 3. A positive sign convention and kinematic hypothesis of the Mindlin's plate

The components u and w of displacements of points of the plate strip, expressed by the displacements of the midsurface $(\bar{u}, \bar{w}, \bar{\alpha})$, equal

$$u(x) = \bar{u}(x) - z\bar{\alpha}(x), \quad (4.1)$$

$$w(x, z) = \bar{w}(x), \quad (4.2)$$

where

$$\bar{\alpha}(x) = \frac{dw}{dx} - \beta. \quad (4.3)$$

The Hook's constitutive equations as well as the Cauchy's equations of the plate strip bent to a cylindrical surface take the form

$$\begin{bmatrix} \sigma_x \\ \tau_{xz} \end{bmatrix} = \begin{bmatrix} \frac{E}{1-\nu^2} & 0 \\ 0 & \frac{E}{2(1+\nu)} \end{bmatrix} \begin{bmatrix} \varepsilon_x \\ \gamma_{xz} \end{bmatrix} = \begin{bmatrix} D_1 & 0 \\ 0 & D_2 \end{bmatrix} \begin{bmatrix} \varepsilon_x \\ \gamma_{xz} \end{bmatrix}. \quad (4.4)$$

$$\begin{bmatrix} \varepsilon_x \\ \gamma_{xz} \end{bmatrix} = \begin{bmatrix} \frac{\partial}{\partial x} & 0 \\ \frac{\partial}{\partial z} & \frac{\partial}{\partial x} \end{bmatrix} \begin{bmatrix} u \\ w \end{bmatrix}. \quad (4.5)$$

Expressing the displacements through the nodal parameters of the element we receive

$$\begin{bmatrix} u(x, z) \\ w(x, z) \end{bmatrix} = \sum_{i=1}^n \begin{bmatrix} N_i & 0 & -zN_i \\ 0 & N_i & 0 \end{bmatrix} \begin{bmatrix} u_i \\ w_i \\ \alpha_i \end{bmatrix}, \quad (4.6)$$

where N_i are the assumed shape functions.

Using equations (4.4)-(4.6) as well as the first member of equation (3.1), we receive a relation describing a block of stiffness matrix of the strip.

$$\mathbf{K}_{ij} = \int_L \int_{-0.5}^{0.5} \int_{-h/2}^{h/2} \left(\begin{bmatrix} N_{i,x} D_1 N_{j,x} & 0 & -N_{i,x} z D_1 N_{j,x} \\ 0 & 0 & 0 \\ -N_{i,x} z D_1 N_{j,x} & 0 & N_{i,x} z^2 D_1 N_{j,x} \end{bmatrix} + \begin{bmatrix} 0 & 0 & 0 \\ 0 & N_{i,x} D_2 N_{j,x} & -N_{i,x} D_2 N_j \\ 0 & -N_i D_2 N_{j,x} & N_i D_2 N_j \end{bmatrix} \right) dz dy dx. \quad (4.7a)$$

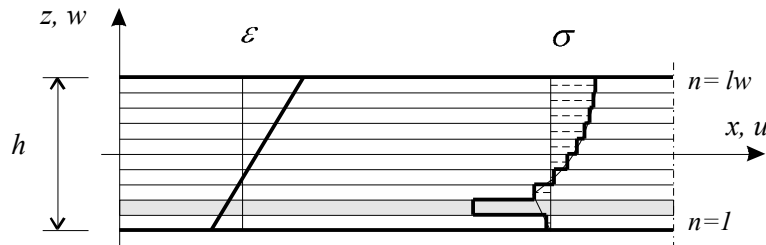


Fig. 4. Strains and displacements in an element with a single layer of reinforcement

Since the element is heterogeneous across the thickness of the plate, the section has been divided into layers, and reinforcing bars have been smeared to appropriate layers of mechanically equivalent thickness – see Fig. 4. There are some reinforcement layers and some concrete matrix layers, the number and the layout of which are arbitrary.

A layered slab model was used to account for the reinforcement. This is a standard approach used in modelling reinforced concrete flexural elements, see e.g. Owen and Figueiras, [28].

Performing the rectangular integration with respect to thickness coordinate (variable z) we receive the final form of the expression determining the block of stiffness matrix of the layer element of the finite strip.

$$\mathbf{K}_{ij} = \int_L \sum_{n=1}^{lw} \left(\begin{bmatrix} N_{i,x} D_1 N_{j,x} & 0 & -N_{i,x} z_n D_1 N_{j,x} \\ 0 & 0 & 0 \\ -N_{i,x} z_n D_1 N_{j,x} & 0 & N_{i,x} \left(z_n^2 + \frac{h_n^2}{12} \right) D_1 N_{j,x} \end{bmatrix} + \begin{bmatrix} 0 & 0 & 0 \\ 0 & N_{i,x} D_2 N_{j,x} & -N_{i,x} D_2 N_j \\ 0 & -N_i D_2 N_{j,x} & N_i D_2 N_j \end{bmatrix} \right) h_n dx \quad (4.7b)$$

In equation (4.7b) summation runs over all the l_w layers of the element. In each layer, parameters D_1 and D_2 correspond with the characteristics of the concrete or the steel, so we received an equation determining the stiffness matrix of the reinforced concrete element.

5. CONSTITUTIVE MODEL OF REINFORCED CONCRETE STRUCTURE

The mathematical model of the reinforced concrete structure consists of a model of concrete in a compressed zone, a concrete model in a tensioned zone, a model of reinforcement and a model of interaction between concrete and reinforcing bars. The layer concept is characterised by subdividing a

finite element across its thickness into several layers. For each of these layers appropriate constitutive relations, for concrete and reinforcement, are used.

5.1. Concrete model in the compressed zone

In the state of a uniaxial compression of the concrete, a simple hyperbolic relation between strain and stress has been assumed after Hofstetter and Mang [2]. It is expressed by the equation.

$$\sigma = \frac{E_0 \varepsilon}{1 + \left(\frac{E_0 \varepsilon_c}{f_c} - 2 \right) \frac{\varepsilon}{\varepsilon_c} + \left(\frac{\varepsilon}{\varepsilon_c} \right)^2} \quad (5.1)$$

where: f_c – compressive strength of concrete, ε_c – strain corresponding with the compressive strength of concrete, E_0 – initial Young modulus of concrete.

In order to determine the value of the irreversible deformations it has been assumed that, the strain consists of an elastic part (reversible) and of a plastic one (irreversible)

$$\varepsilon = \varepsilon_e + \varepsilon_p. \quad (5.2)$$

Substituting (5.2) into (5.1) and solving the equation with respect to ε_p , we receive relations presenting values of the irreversible strains, respectively for $\varepsilon > \varepsilon_c$, (sign +) and $\varepsilon \leq \varepsilon_c$ (sign -) where:

$$\varepsilon_p = \frac{1}{2E_0 f_c \sigma} \left(2E_0 \varepsilon_c f_c \sigma - 2E_0^2 \varepsilon_c^2 \sigma - 2f_c \sigma^2 + 2E_0^2 \varepsilon_c^2 f_c \right. \\ \left. \pm \sqrt{E_0^4 \varepsilon_c^4 \sigma^2 - 4E_0^3 \varepsilon_c^3 \sigma^2 f_c - 2E_0^4 \varepsilon_c^4 \sigma f_c + 4E_0^3 \varepsilon_c^3 \sigma f_c^2 + E_0^4 \varepsilon_c^4 f_c^2} \right) \quad (5.3)$$

5.2. Concrete model in the tensioned zone

The response of concrete under tensile stresses is assumed to be linear elastic until formation of a crack ($\varepsilon = \varepsilon_r$) Fig. 5. The cracked material is treated as a continuum allowing damage to be spread or smeared over the region associated with a sampling node for numerical integration over the volume of a finite element. The phenomenon is described in terms of stress – strain relations.

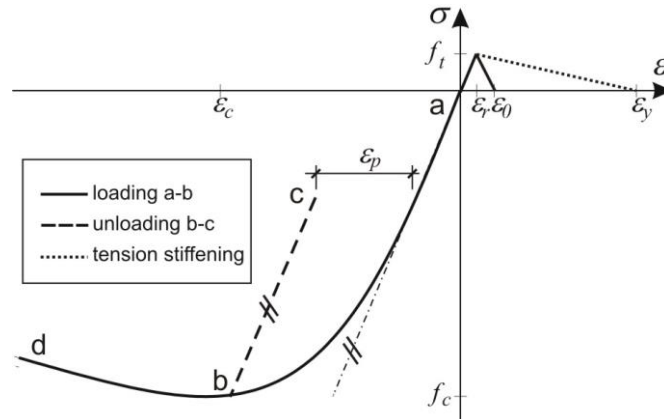


Fig. 5. Schematic representation of constitutive model of concrete

To overcome mesh sensitivity effect resulting from continuous treatment of geometrical discontinuity, fracture energy G_f is used as an additional material parameter Karihaloo [29]. The stiffness in the strain softening region is described by the equation

$$E_r = E \left(1 - \frac{2EG_f}{l_s f_r^2} \right)^{-1} \quad (5.4)$$

where l_s is the element size, equal the width of the crack band, f_r is the tensile strength of concrete.

5.3. Concrete – reinforcement interaction model

The usage of smeared representation of concrete cracking, results in implicit modelling of concrete – reinforcement interface behaviour as well as aggregate interlock of cracked concrete by modifying the constitutive relations for concrete.

Due to bond effects, cracked concrete carries a certain amount of tensile stress between cracks. The concrete adheres to the reinforcing bars and contributes to the overall stiffness of the structure. The effect is known as tension stiffening.

The behaviour of cracked reinforced concrete loaded in tension can be considered as a superposition of stiffness of plain concrete and additional stiffness due to bonds between concrete and reinforcement, c.f. dot line, Fig. 5.

Aggregate interlock at cracks is modelled by a modified shear modulus G according to Fig. 6.

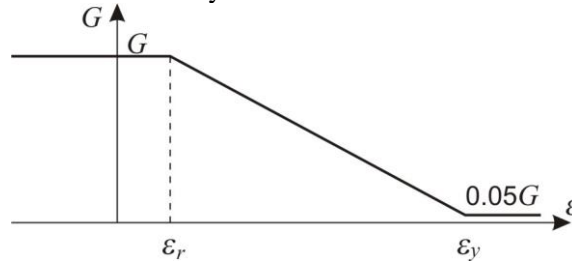


Fig. 6. Modification of shear modulus of concrete in tensioned zone

Tension stiffening and aggregate interlocking effects are assumed to vanish while initiating reinforcement yielding ($\varepsilon = \varepsilon_y$).

5.4. Model of reinforcement

The reinforcing bars are considered as steel layers of equivalent thickness. Each steel layer has an uniaxial behaviour resisting only the axial force in the bar direction. A bilinear idealisation is adopted in order to model the elasto-plastic stress – strain relationship. The steel initially deforms according to the elastic modulus E_s , until the strain level reaches a uniaxial yield strain ε_y . Linear strain-hardening response, characterised by the modulus E_H , describes the material behaviour after further load.

6. INTERFACE ELEMENT

6.1. Element formulation

The interface elements serve two aims in the considered problem:

- connect finite elements of different nodal parameters (translational degrees of freedom of subsoil elements as well as translational and rotational degrees of freedom of the plate Fig. 7),

- model adhesion and slide zones on the foundation – subsoil contact area.

It has been assumed that there is consistency between the displacements of the nodes of the interface element and the displacements of a given surface of the plate (upper nodes) and the displacements of the subsoil (lower nodes):

$$\begin{aligned} u^g(x) &= u^b(x) + \frac{h}{2} \alpha^b(x) \\ w^g(x) &= w^b(x) \end{aligned} \quad (6.1a)$$

$$\begin{aligned} u^d(x) &= u^s(x) \\ w^d(x) &= w^s(x) \end{aligned} \quad (6.1b)$$

In case of linear elasticity between mutual reactions $\{t_c\}$ and displacements $\{\Delta u\}$ on the contact area the following relation takes place

$$\begin{bmatrix} \tau \\ \sigma_n \end{bmatrix} = \begin{bmatrix} k_t & 0 \\ 0 & k_n \end{bmatrix} \begin{bmatrix} \Delta u_t \\ \Delta u_n \end{bmatrix} \quad (6.2)$$

where k_s and k_n are the coefficients of elasticity respectively for tangential and normal directions.

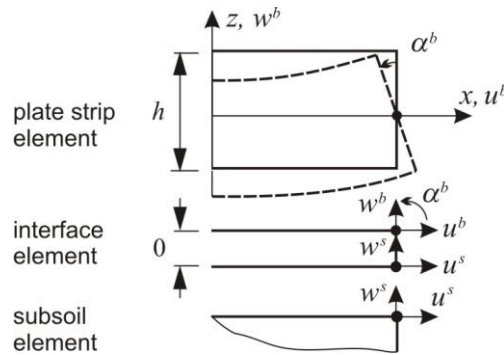


Fig. 7. The interface element connecting the plate and the subsoil elements

Applying (6.1), the displacements of upper and lower nodes can be expressed by nodal parameters of the plate respectively

$$\mathbf{u}^g = \begin{bmatrix} u^g(x) \\ w^g(x) \end{bmatrix} = \sum_{i=1}^n \begin{bmatrix} N_i & 0 \\ 0 & N_i \end{bmatrix} \begin{bmatrix} \frac{h}{2} N_i \\ 0 \end{bmatrix} \begin{bmatrix} u_i^b \\ w_i^b \\ \alpha_i^b \end{bmatrix} \quad (6.3)$$

and nodal parameters of the subsoil element.

$$\mathbf{u}^d = \begin{bmatrix} u^d(x) \\ w^d(x) \end{bmatrix} = \sum_{i=1}^n \begin{bmatrix} N_i & 0 \\ 0 & N_i \end{bmatrix} \begin{bmatrix} u_i^s \\ w_i^s \end{bmatrix} \quad (6.4)$$

Presenting the difference between the upper and the lower nodal displacements in the form

$$\Delta \mathbf{u} = \mathbf{u}^g - \mathbf{u}^d = \mathbf{N} \mathbf{u}^{bs} \quad (6.5)$$

and substituting (6.5) and (6.2) into the second component of the virtual work equation (3.1), we receive a relation defining a stiffness matrix of the interface element

$$\mathbf{K}_k = \int_0^L \mathbf{N}^T \mathbf{D} \mathbf{N} dx \quad (6.6)$$

In order to enable modelling the zones of adhesion and the slide zones, the elasticity matrix $[D]$, defined by equation (6.2) will be replaced with a relevant elasto-plastic matrix.

6.2. An elasto-plastic contact model

Within the area of the foundation and the subsoil we can distinguish a full adhesion zone of both bodies and a sliding zone. An isotropic Coulomb friction model has been used

$$f = |\tau| + \sigma \operatorname{tg} \phi - c, \quad (6.7)$$

where: ϕ is an internal friction angle and c – cohesion, Fig. 8.

Taking the advantage of the analogy between a friction phenomenon and the flow theory of plasticity, the problem of the nodes on the foundation – subsoil contact area has been reduced to a substitute elasto-plastic problem.

The vector of displacement differences between upper and lower contact area $\{\Delta u\}$ given in equation (6.5) can be regarded as a measure of strains of the interface element. By analogy with a tensor of a total velocity of strains in the flow theory of plasticity, the vector $\{\Delta u\}$ can be expressed as a sum of velocities of elastic strains and plastic slides velocities.

$$\Delta \dot{\mathbf{u}} = \Delta \dot{\mathbf{u}}_e + \Delta \dot{\mathbf{u}}_p. \quad (6.8)$$

Equation (6.7) can be regarded as plasticity condition (the condition of sliding of the foundation on the subsoil surface). The elasto-plastic matrix of the interface element takes the general form

$$\mathbf{D}_{ep} = \mathbf{D} - \frac{\mathbf{D} \frac{\partial g}{\partial \boldsymbol{\sigma}} \left(\frac{\partial f}{\partial \boldsymbol{\sigma}} \right)^T}{\left(\frac{\partial f}{\partial \boldsymbol{\sigma}} \right)^T \mathbf{D} \frac{\partial g}{\partial \boldsymbol{\sigma}}}, \quad (6.9)$$

where g is a scalar function of stresses, determining the plastic potential in the plastic flow rule.

Considering the flow rule associated with plasticity condition, the elasto-plastic matrix is described by the equation

$$\mathbf{D}_{ep} = \frac{k_s k_n}{k_s + k_n \operatorname{tg}^2 \phi} \begin{bmatrix} \operatorname{tg}^2 \phi & -\operatorname{tg} \phi \\ -\operatorname{tg} \phi & 1 \end{bmatrix}. \quad (6.10)$$

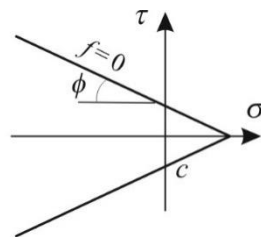


Fig. 8. Coulomb's friction condition

7. THE SUBSOIL FINITE ELEMENT

The Serendipity element has been used to model the subsoil in the plane state of strains. The reduced integration scheme has been applied by Zienkiewicz and Taylor [30].

To reduce dilation in the soil while plastic flow, a non-associated flow rule has been used. A plastic potential function connected with the Mohr-Coulomb's plasticity condition has been used in an analogous form substituting the internal friction angle of the soil with a dilation angle. The elasto-plastic matrix of the subsoil element is defined by equation (6.9).

8. SOLUTION STRATEGY OF A NON-LINEAR FEM PROBLEM

8.1. An incremental-iterative method of solving the non-linear task

The following linearised system of equilibrium equations is solved in each incremental step Δt

$$\mathbf{K}_T \Delta \mathbf{r} = {}^{t+\Delta t} \mathbf{F}_{ext} - {}^t \mathbf{F}_{int} \quad (8.1)$$

where \mathbf{K}_T is a tangential stiffness matrix of the whole system, \mathbf{F}_{ext} is an external nodal load vector, \mathbf{F}_{int} is an internal force vector, $\Delta \mathbf{r}$ is a vector of increments of generalised node displacements.

Due to the applied non-associated flow rule in subsoil elements, the modified Newton-Raphson's method has been used ($\mathbf{K}_T = \mathbf{K}_0$, Fig. 9).

For subsoil elements and contact elements an incremental formulation has been applied. On the basis of increments of generalised node displacements, derived from (8.1), strain increments have been calculated and next, using (6.9) or (6.10), stress increments have been obtained.

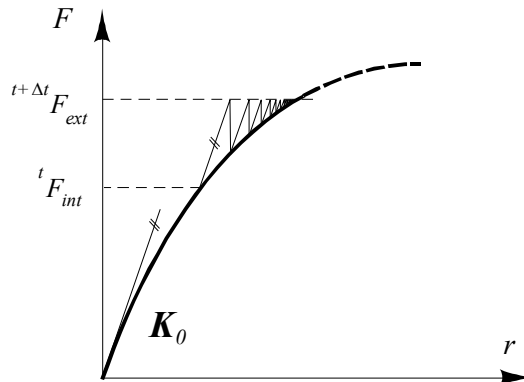


Fig. 9. A modified Newton-Raphson's method for a system of one-degree of freedom

A total formulation has been used for structure elements, where the total displacements and the total strains have been derived from displacement increments. Total stresses have been calculated on the basis of the total strains from the equation $\boldsymbol{\sigma} = \mathbf{D}(\boldsymbol{\varepsilon}) \boldsymbol{\varepsilon}$ (e.g. for the layers of compressed concrete, see (5.1)). Using the elaborated mathematical model computer programmes have been prepared. The programs are prepared for the analysis of the soil – reinforced concrete structure interaction in a plain strains state.

9. VERIFICATION OF THE MODEL

In order to check the correctness of the computer programme solutions the results of three tests are presented. Since the literature does not describe any experimental or numerical tests taking into account

the structure stiffness degradation, the influence of subsoil and contact conditions, which would match the elaborated model, the author has decided to carry out separate tests for particular parts of the model. The numerical solutions are compared to the analytical solutions as well as the results of laboratory experiments.

9.1. Test 1 – The Sadowsky’s problem

Contact pressures under the punch intended into an elastic half-plane achieved in an analytical solution are compared with numerical results (Fig. 10). FEM solution achieved in a full integration of the stiffness matrix of the interface element shows oscillation of the contact pressures. This can be limited applying a reduced Newton-Cotes’s integration, leading to the stiffness matrix diagonalisation c.f. Hohberg [31].

9.2. Test 2 – The Monnier’s reinforced concrete beam

In order to verify the elaborated reinforced concrete model, the numerical solutions have been compared with the experiment results by Monnier [32] (see Fig. 11).

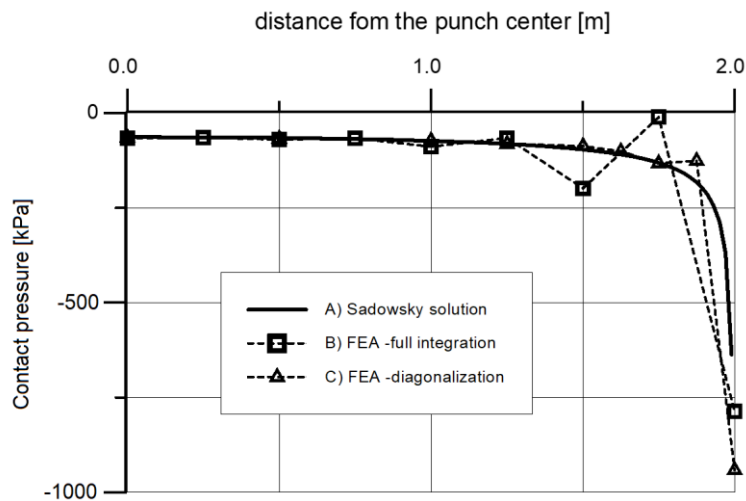


Fig. 10. Diagram of the contact pressures under the punch

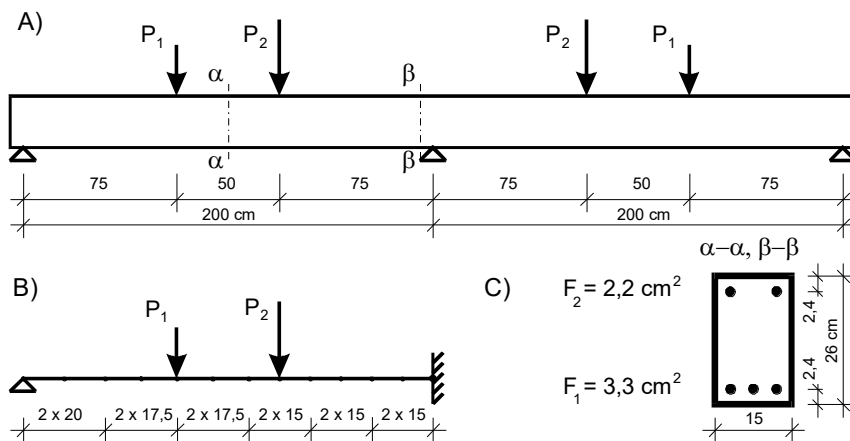


Fig. 11. A) A beam geometry, B) FE discretisation, C) reinforcement distribution

Each element has been divided into 11 layers in the vertical direction, which the second and the tenth ones are the reinforcement layers. The values of the deflection of the section $\alpha\text{-}\alpha$ achieved in the measurements are compared to linear and non-linear FEM solutions (Fig. 12).

It can be stated that there is a considerable consistency between the non-linear solution and the results of the Monnier's test, which proves the correctness of the elaborated numerical model of the reinforced concrete.

9.3. Test 3 – Verification of a non-linear contact model

The numerical solution is compared to the experimental results by Zong-Ze et al. [33], in which deformations in the concrete – soil contact area have been investigated. In the experiment, a direct shear apparatus has been applied as well as a concrete plate 60 cm long, with viziery and measuring instruments installed inside it. A sample of the soil placed in the apparatus was moved along the surface. As the mean shear stresses τ arise, caused by a horizontal force which moves the sample, successive points of the soil, starting from point No 6 situated near the edge, are displaced. Displacements of 6 points of the soil as well as displacements of the edge of the shearing apparatus relatively to the concrete plate are presented in Fig. 13a. The results of numerical simulation of the experiments are presented on Fig. 13b.

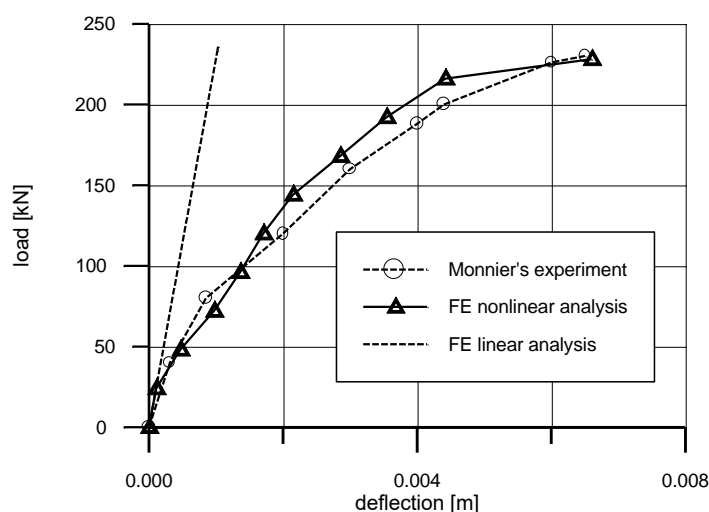


Fig. 12. A diagram of the load-deflection relation of a section α of a beam

The comparison of the two figures reveals that the elaborated interaction model represents the behaviour of the apparatus well, but it is worse as far as the behaviour of the particular points of the contact area are concerned, especially in the centre of the soil sample.

10. RECOMMENDED SET OF FINITE ELEMENTS

After a series of numerical tests (three of them are presented above), in which various finite elements and integration schemes have been applied, the following set of elements (Fig. 14) give satisfactory results:

- 3-node quadratic Lagrangian layered element. Selective Gauss-Legendre integration procedure was used in longitudinal direction, to eliminate undesirable phenomenon which is referred to as shear locking c.f. Zienkiewicz and Taylor [30]. The procedure consists of applying a reduced integration

rule to evaluate the stiffness matrix parts associated with shear strain energy and full integration for the remaining terms of the stiffness matrix. Taking into account the form of integrated function with respect to thickness coordinate, rectangular rule was performed c.f. Bergan [34].

- 6-node quadratic Lagrangian zero thickness interface element. Reduced order Newton-Cotes integration rule was employed to limit oscillation of contact pressures under the foundation c.f. test 1.
- 8-node quadratic Serendipity subsoil element. Reduced Gauss-Legendre quadrature was used c.f. Sloan and Randolph [35].

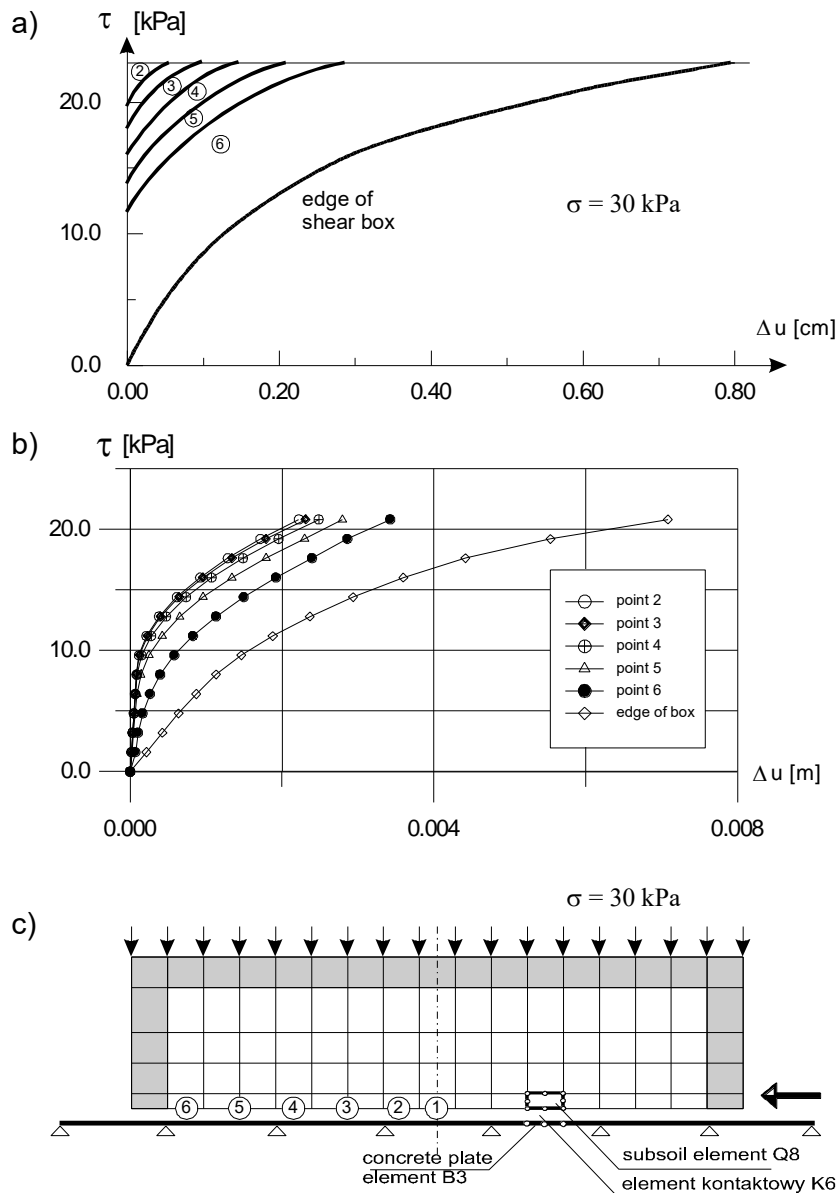


Fig. 13. The contact model verification: a) the Zong-Ze et al. [33] experiment results, b) results of numerical simulation, c) loads and spatial discretisation of the system

11. SUMMARY AND CONCLUSIONS

The paper presents an elaborated model of interaction between a structure and subsoil in plane strain conditions. The model enables static analysis of reinforced concrete structures supported by deformable subsoil with arbitrary system of geological layers under monotonic loads. The analysis consider the possibility of slip of the foundation along the subsoil surface. The contact model enables identification of slide and adhesion zones. In the nonlinear reinforced concrete structure model the following features are considered: crack creation in the tensioned zone, yielding of reinforcement, creation of irreversible strains in reinforcement and concrete, nonlinear stress distribution in the compression zone as well as the concrete – reinforcement interaction. The elasto-plastic model of the subsoil with non-associated flow rule prevents the continuum from dilation while yielding.

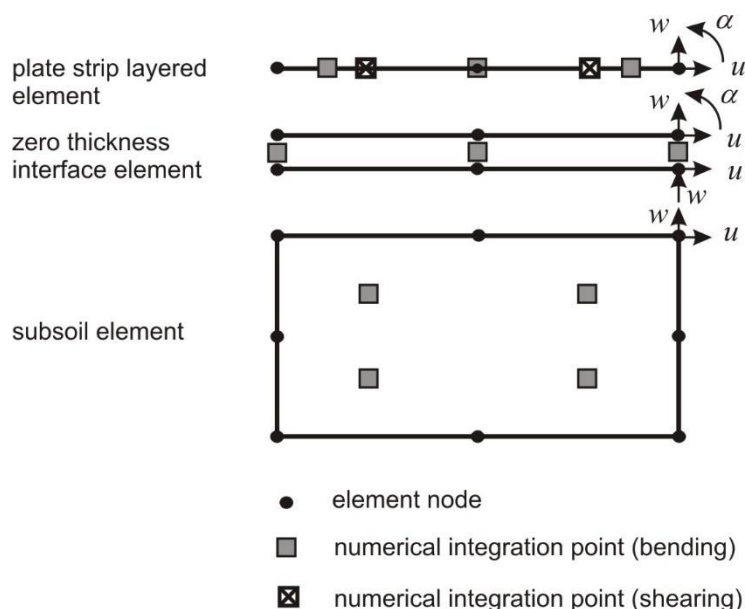


Fig. 14. The recommended set of finite elements

The elasto-plastic approach has been used to describe processes taking place in the subsoil and the reinforced concrete structure.

The problem of constraints as well as the phenomena taking place at the contact area have been simulated by equivalent problem of elasto-plasticity. Such a description has simplified the task considerably. The formulation enabled receiving the solution with the use of elaborated computer program.

A set of finite elements has been composed to model the subsoil (8-node quadratic Serendipity element), the reinforced concrete structure (3-node quadratic Lagrangian layered element) and the interface (6-node quadratic Lagrangian zero thickness element). The proposed contact element enables connecting elements with different nodal degrees of freedom: translational for the subsoil, translational and rotational for the foundation raft.

An important advantage of the prepared numerical model is the fact that it requires only a small number of mostly standard material parameters, values of which are used in everyday design.

In the described set of finite elements, the method of numerical integration of individual stiffness matrices plays a very important role. In the numerical model of the RC plate, reduced integration rule for shear terms, full integration for bending terms and rectangular rule for integration with respect to the plate thickness are proved to be effective. In the case of the interface element, the use of the reduced

Newton-Cotes integration rule minimizes the undesirable phenomenon of contact stress oscillations. The use of reduced Gauss-Legendre quadratures integration of the soil element (8-node Serendipity), widely described in the literature, confirmed its effectiveness in the elastio-plastic solutions.

The individual components of the set of elements have been validated. The distribution of contact stresses in the Sadowsky's test, the deflection of the RC Monnier's beam and the soil – concrete contact in the direct shear apparatus were examined. The results turned out to be satisfactory. It would be advisable to validate the entire set of elements for problems containing an RC slab supported on the subsoil. However, finding such a benchmark that would enable the identification of the values of the parameters used in the proposed numerical model is a future challenge.

REFERENCES

1. Look, BG 2007. *Handbook of geotechnical investigation and design tables*. London: Taylor & Francis.
2. Hofstetter, G and Mang, HA 1995. *Computation mechanics of reinforced concrete structures*. Wiesbaden: F. Vieweg & Sohn Verlagsgesellschaft mbH.
3. Tejchman, J and Bobiński, J 2013. *Continuous and discontinuous modelling of fracture in concrete using FEM*. Heidelberg: Springer.
4. Chen, WF and Mizuno, E 1990. *Nonlinear analysis in soil mechanics: Theory and implementation*. Amsterdam: Elsevier.
5. Yu, HS 2006. *Plasticity and geotechnics*. Berlin: Springer.
6. Puzrin, AM 2012. *Constitutive modelling in geomechanics. Introduction*. Berlin: Springer.
7. Meschke, G, Pichler, B and Rots, JG 2022. *Computational modelling of concrete and concrete structures*. Boca Raton: CRC Press/Balkema.
8. Michałowski, R and Mróz, Z 1978. Associated and non-associated sliding rules in contact friction problems. *Archives of Mechanics* **30**, 3, 259-276.
9. Potts, DM and Zdravković, L 2001. *Finite element analysis in geotechnical engineering: Applications*, London: Thomas Telford.
10. Sheng, D, Wriggers, P and Sloan, SW 2007. Application of frictional contact in geotechnical engineering. *Int. J. of Geomechanics* **7**, 3, 176-185.
11. Dhadse, GD, Ramtekkar, G and Bhatt, G 2022. Influence due to interface in finite element modeling of soil-structure interaction system: a study considering modified interface element. *Research on Engineering Structures & Materials* **8** 1, 127-154.
12. Goodman, RE, Taylor, RL and Brekke, TL 1968. A model for the mechanics of jointed rock. *Journal of the Soil Mechanics and Foundations Division* **94**, 3, 637-659.
13. Desai, CS, Zaman, MM, Lighter, JG and Siriwardane, HJ 1984. Thin-layer element for interfaces and joints. *Int. J. Num. Anal. Meth. Geomech.* **8**, 1, 19-43.
14. Qian, XX, Yuan, HN, Li, QM and Zhang BY 2013. Comparative study on interface elements, thin-layer elements, and contact analysis methods in the analysis of high concrete-faced rockfill dams. *Journal of Applied Mathematics* **2013**, 1-11.
15. Damians, IP, Yu, Y, Lloret, A and Bathurst, RJ 2015. Equivalent interface properties to model soil-facing interactions with zero-thickness and continuum element methodologies. *From Fundamentals to Applications in Geotechnics*, 1065-1072.
16. Dalili, SM, Huat, BBK, Jaafar, MS and Alkarni, A 2015. Soil – framed structure interaction analysis – a new interface element. *Latin American J. of Solids Struct* **12**, 2, 226-249.

17. Li, Y-K, Han, X-L, Ji, J, Fu, D-L, Qiu, Y-K, Dai, B-C and Lin, C 2015. Behavior of interfaces between granular soil and structure: A state-of-the-art review. *The Open Civil Engineering Journal* **9**, 213-223.
18. Dhadse, GD, Ramtekkar, G and Bhatt, G 2021. Finite element modeling of soil structure interaction system with interface: a review. *Archives of Computational Methods in Engineering* **28**, 5, 3415-3432.
19. Belhadj, FZ, Belhadj, AF and Chabaat, M. 2022. Soil-structure interaction interfaces: literature review. *Arabian Journal of Geosciences* **15**, 1130.
20. Chen, X, Zhang, J, Xiao, Y and Li, J 2015. Effect of roughness on shear behavior of red clay – concrete interface in large-scale direct shear tests. *Can. Geotech. J.* **52**, 1122-1135.
21. Zhang, G, Liang, D and Zhang, JM 2006. Image analysis measurement of soil particle movement during a soil–structure interface test. *Computers and Geotechnics*, **33**, 4-5, 248-59.
22. Zhang, G and Zhang, J 2009. State of the art: Mechanical behavior of soil – structure interface. *Progress in Natural Science* **19**, 1187-1196.
23. Hu, L and Pu, J 2004. Testing and modeling of soil-structure interface. *J. Geotech. Geoenviron. Eng.* **130**, 8, 851-860.
24. DeJong, JT and Westgate, ZJ 2009. Role of initial state, material properties, and confinement condition on local and global soil – structure interface behavior. *J. Geotech. Geoenviron. Eng.* **135**, 11, 1646-1660.
25. Dang, HK and Meguid, MA 2013. An efficient finite–discrete element method for quasi-static nonlinear soil–structure interaction problems. *Int. J. Numer. Anal. Meth. Geomech.* **37**, 130-149.
26. Carbonell, JM, Monforte, L, Ciantia, LM, Arroyo, M and Gens, A 2022. Geotechnical particle finite element method for modeling of soil – structure interaction under large deformation conditions. *Journal of Rock Mechanics and Geotechnical Engineering* **14**, 967-983.
27. Koiter, WT 1960. General theorem for elastic-plastic solids. In: Snedon, IN and Hill, R (eds) *Progress in solid mechanics*. Amsterdam: North Holland, **1**, 165-221.
28. Owen, DR and Figueiras, JA 1984. Ultimate load analysis of reinforced concrete plates and shells including geometric nonlinear effects. In: Hinton, E and Owen, DR (eds) *Finite element software for plates and shells*. Swansea: Pineridge Press, 327-382.
29. Karihaloo, BL 1995. *Fracture mechanics and structural concrete*. Harlow: Longman Scientific & Technical.
30. Zienkiewicz, OC and Taylor, RL 1991. *The finite element method*. Vol. 2 *Solid and fluid mechanics, dynamics and non-linearity*. London: McGraw-Hill, 4th ed.
31. Hohberg, J-M 1990. A note on spurious oscillations in FEM joint elements, *Earthquake Engng. Struct. Dyn.* **19**, 773-779.
32. Monnier, T 1970. The behavior of continuous beams in reinforced concrete, *Heron* **17**, 1, 1-83.
33. Zong-Ze, Y, Hong, Z and Gua-Hua, X 1995. A study of deformation in the interface between soil and concrete. *Comp. & Geotech.* **17**, 75-92.
34. Bergan, PG 1984. Some aspects of interpolation and integration in nonlinear finite element analysis of reinforced concrete structures, In: Damjančić, F et al. (eds) *Computer-Aided Analysis and Design of Concrete Structures*. Swansea: Pineridge Press, 301-316.
35. Sloan, SW and Randolph, MF 1982. Numerical prediction of collapse loads using finite element method, *Int. J. Num. Anal. Meth. Geomech.* **6**, 47-76.